Pressure Effect on the Optical Bandshape of Solid Oxygen

Sergey Medvedev,[†,||] Mario Santoro,[‡,⊥] Federico Gorelli,[‡,⊥] Yuriy Gaididei,[§] Vadim Loktev,[§] and Hans J. Jodl*[,†,‡]

Fachbereich Physik, Universität Kaiserslautern, Kaiserslautern, Germany, LENS, European Laboratory for Nonlinear Spectroscopy, Florence, Italy, Bogolyubov Institute of Theoretical Physics, Kiev, Ukraine, National Technical University "Kharkov Polytechnical Institute", Kharkov, Ukraine, and INFM, National Institute for the Physics of Matter, Italy

Received: January 24, 2003; In Final Form: March 25, 2003

The magnetism in solid oxygen, especially in different high-pressure phases, is not completely understood but can be studied indirectly by spectroscopic techniques. Therefore, we measured and modeled pressure effects on the optical band shape of vibronic two-molecule transitions $^3\Sigma_g^-{}^3\Sigma_g^- \rightarrow {}^1\Delta_g{}^3\Sigma_g^-$. Corresponding spectra at ambient and elevated ($P < 10$ GPa) hydrostatic pressure and low temperature were very complex but could be clearly assigned to a zero phonon line (ZPL), which in solid oxygen is presented by the exciton−magnon doublet, and its phonon sideband. After the deconvolution of the spectra (ZPL and sideband), the frequency and integrated intensity of the band origin were plotted as functions of pressure. We tried to develop a theory and to model the combined excitation (exciton + magnon + phonons); then we could derive theoretical relations that we compared to experimental data: (i) the splitting of the exciton−magnon doublet increases with pressure because of the growth of all (resonance and exchange) interactions in the basal *ab*-plane; (ii) the integrated intensity of the ZPL decreases with pressure because the equilibrium positions of molecular oscillators in the ground and optically excited crystal states are shifted relative to each other; (iii) the total band intensity increases with pressure as the combined excitations are assisted by intermolecular exchange interaction due to the decrease in the distance between molecules participating in this transition.

1. Introduction

To perform studies on magnetism at high pressure is not a trivial task; we know of only one publication in which the authors directly measure the pressure dependence of magnetic susceptibility at ultrahigh pressure in a diamond anvil cell.[1] The derived quantity (e.g., exchange integral J in the expression for the spin−spin intermolecular interaction) is very pressure-sensitive and can be modeled theoretically in a straightforward way as a function of distance between molecular spins. Therefore, we had chosen an indirect way—via optical spectroscopy—to study the magnetic high-pressure phases of solid oxygen at low temperatures. Spectroscopic characteristics, such as mode frequency or band intensity, contain important information about this magnetic interaction within one crystal phase or at the phase transition; of course this type of interaction must be separated from other types of contributions (phonon−phonon, etc.).

Solid oxygen, as it is well known, is a unique crystal. It combines the properties of a cryocrystal and a magnet; it transforms from transparent to colored at increasing pressure,[2] becomes a metallic molecular crystal,[3] and even transforms into a superconducting state at higher pressure.[4] These unusual features originate from pecularities in the electronic structure of the O_2 molecule such as a nonzero electronic spin in its triplet ground state $^3\Sigma_g^-$and two low-lying singlet electronic levels ($^1\Delta_g$ and $^1\Sigma_g^+$ at ∼8000 cm^{-1} and at ∼13 000 cm^{-1}) above the ground state. Therefore, these electronic spectra contain information not only on magnetic interactions but also, because of the complexity of combined transitions (exciton or exciton/vibron plus magnon, plus phonon), on other types of interaction when studied as a function of pressure and temperature.

To our knowledge, there are two earlier experimental publications: ref 2, concerning the double transitions $^3\Sigma^3\Sigma \rightarrow {}^1\Sigma^1\Sigma$ and $^3\Sigma^3\Sigma \rightarrow \Delta\Delta$ above 12 000 cm^{-1} in solid oxygen during the $\beta \rightarrow \delta \rightarrow \epsilon$ phase transition, and ref 5 by Loktev, who using these data tried to predict polarization properties of double-molecule optical bands in δ- and ϵ-phases. Recently, Medvedev et al. studied carefully the transition $^3\Sigma_g^-{}^3\Sigma_g^- \rightarrow {}^1\Delta_g{}^3\ \Sigma_g^-$ at ∼8000 cm^{-1} in solid oxygen at ambient pressure and low temperatures,[6] whereas Santoro et al. investigated the same transition in compressed oxygen ($P < 10$ GPa).[7]

With respect to the magnetism in solid oxygen phases, we would like to quote two recent papers that are of certain relevance to our discussion (see later). Gorelli et al. proved by IR spectroscopy the antiferromagnetism of the δ-phase and interpreted the molecular vibrational coupling by the exchange integral J.[8] Santoro et al. determined from electronic spectra this exchange integral J between nearest-neighbor molecules as a function of pressure from the α-phase up to 7 GPa.[7]

The relevant oxygen phases for our investigations are the α-, β-, δ-, and ϵ- phases (see review, ref 9), in short, what is necessary for the following consideration: the monoclinic α-phase exists at ambient pressure below $T \leq 24$ K and possesses a structural space group of $C2/m$ with one molecule in the primitive crystallographic cell but with two in the magnetic primitive cell with antiferromagnetic order. The

* To whom correspondence should be addressed. E-mail: jodl@physik.uni-kl.de. Fax: ++49 (0)631 205-3677.
† Universität Kaiserslautern.
‡ European Laboratory for Nonlinear Spectroscopy.
§ Bogolyubov Institute of Theoretical Physics.
|| National Technical University "Kharkov Polytechnical Institute".
⊥ National Institute for the Physics of Matter.

10.1021/jp0342024 CCC: $25.00
Published on Web 04/29/2003

intermolecular pair potential (van der Waals and electrostatic term) for collinear molecules has a minimum of about 270 K, whereas the additional contribution by exchange interaction is about 30 K. The long-range orientational and spin orders are mainly governed by a spin−spin exchange interaction. The rhomohobedral β-phase exists in a wider pressure (P < 10 GPa)−temperature (T > 24 K) range and possesses a structural space group of $R\bar{3}m$ with one molecule in the nonmagnetic unit cell. The magnetic state of this phase is described nowadays as a quasi-2D frustrated 120° triangular lattice (three spin sublattices with the Loktev structure) antiferromagnet. The orthorhombic δ-phase is a low-temperature (T < 200 K), high-pressure phase situated between the α- and ϵ-phases. Gorelli et al. recently presented X-ray diffraction results for pressures <10 GPa and temperatures <300 K.[10] They confirmed the structural space group *Fmmm* with one molecule per primitive cell. Careful analysis of the raw data demonstrates the similarity of the δ-phase to the α-phase with respect to structure and magnetic behavior. The δ-phase should exist between P = 5.5 and 7.8 GPa at T = 15 K, a temperature that is relevant here. The monoclinic ϵ-phase exists above 7−10 GPa in a wide temperature range; the tentative factor group $A2/m$ with eight molecules per unit cell is in accordance with structural and spectroscopic investigations, known up to now. On the basis of IR and Raman data, Gorelli et al. claim this phase to be nonmagnetic and to be composed of a diamagnetic O_4 entity.[11] The possibility of such a structure was recently confirmed by numerical calculations resulting in *Cmcm* crystal symmetry with rather strongly coupled O_2-O_2 singlet pairs.[12]

The results of the two recent papers on the $^3\Sigma_g^-{}^3\Sigma_g^- \rightarrow {}^1\Delta_g{}^3\Sigma_g^-$ transition, which will be modeled here, are the following: Medvedev et al. analyzed this $^3\Sigma^3\Sigma \rightarrow \Delta^3\Sigma$ transition as a function of temperature at ambient pressure.[6] On the basis of an unambiguous assignment of these electronic spectra and a deconvolution of the band intensity into phononless or ZPL components (i.e., exciton plus magnon line) and its phonon sideband, the frequency of the exciton−magnon transition as a function of temperature was determined. The frequency jump at the $\alpha-\beta$ phase transition is attributed to the additional exchange interaction appearing in the α-phase, and the value for the exchange integral J at ambient pressure was determined. Santoro et al. performed the analysis at higher hydrostatic pressure (P < 12 GPa, T = 14−300 K).[7] From the same frequency jump at the $\alpha-\beta$ and the $\delta-\beta$ phase transitions, the authors determined the exchange integral J as a function of the nearest-neighbor distance (from its pressure dependence) and confirmed in addition the antiferromagnetism of the δ-phase. In both investigations,[6,7] mainly the frequency of this $^3\Sigma^3\Sigma \rightarrow \Delta^3\Sigma$ transition was used rather than the dramatic change in band intensities with increasing pressure. (See Figure 1.) In a naive picture, one may expect an increase in magnetic influence on these complex spectra (exciton + magnon + vibron + phonon) with increasing pressure (i.e., reducing the distance between the spins of interacting oxygen molecules).

Therefore, the aim of this paper is to understand the change in band intensities with pressure and temperature and to model pressure effects on the band shape of the $^3\Sigma^3\Sigma \rightarrow \Delta^3\Sigma$ exciton−magnon transition. In the next section, we will describe briefly the experimental procedure, introduce relevant spectra, and present their evaluation with respect to the band intensity $I(P)$ of the exciton−magnon transition as a function of pressure. In the third section, we will present our model, starting with a proper Hamiltonian and ending with a dependence $I(P)$. At last, in the final section, we will compare experimental and theoretical values.

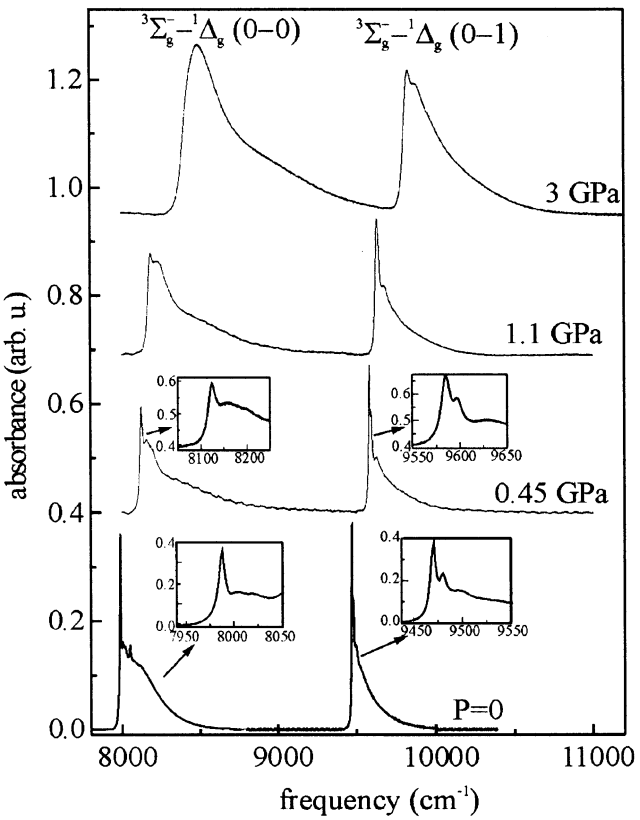

Figure 1. Absorption spectra along the isothermal scan in the near-infrared region showing $^3\Sigma_g^- \rightarrow {}^1\Delta_g$(0−0), (0−1) bands. Details of the exciton−magnon splitting are magnified in the insets.

2. Experimental Set-Up and Results

In both types of experimental investigations (at ambient pressure and at elevated pressure), we used oxygen gas of 99.998% purity. At ambient pressure, the sample was prepared in a specially designed optical cell with diamond windows (thickness 1.2 mm, diameter 10 mm) and was cooled very slowly at phase transitions with large volume changes (liquid → γ → β → α).[6] At high pressure, the sample was prepared in an MDAC via cryoloading and treated in the following way (path through $P-T$ diagram): to avoid the $\gamma-\beta$ phase transition ($\Delta V/V$ ca. −5%), the sample was pressurized to 6 GPa; then pressure and temperature were lowered in such a way that the sample always remained in the β-phase.[7] Several isothermal scans were performed around T = 14 K from ambient pressure up to 11.5 GPa. Isobaric cooling and heating cycles between 15 K and room temperature have been performed at 1.2, 4.1, 5.5, and 6.0 GPa. Altogether, six different samples were studied.

Spectra were recorded in both studies ($P \approx 0$, $P > 0$) by a Fourier spectrometer (Bruker IFS 120 HR). A tungsten lamp and two sets of beam splitters with suitable detectors were used: Si on CaF_2 or quartz as the beam splitter and a liquid-N_2-cooled InSb detector for the range 1900−10 000 cm^{-1}; a dielectric coating on quartz as the beam splitter and a Si diode as the detector for the range 8000−20 000 cm^{-1}. Details of our optical setup for FTIR measurements with an MDAC have been carefully described elsewhere.[13]

The optical quality of spectra in P = 0 studies was controlled in determining the bandwidth of the $^3\Sigma_g^- \rightarrow {}^1\Sigma_g^+$ (∼13 100 cm^{-1}) transition, which was about 1 cm^{-1}. Figure 1 presents

spectra at 14 K at ambient pressure[6] and at elevated pressure.[7] Remarkable are (i) the detailed fine structure, (ii) the asymmetry of bands, and (iii) the changes with pressure (i.e., the loss of fine structure and the increase in band intensity). According to the literature,[14] the two bands are confidently assigned to the electronic (exciton−magnon) $^3\Sigma_g^-(v=0)\,^3\Sigma_g^-(v=0) \rightarrow {}^1\Delta_g(v=0)^3\Sigma_g^-(v=0)$ transition at about 8000 cm^{-1} and to the (exciton + vibron − magnon) $^3\Sigma_g^-(v=0)\,^3\Sigma_g^-(v=0) \rightarrow {}^1\Delta_g(v=1)\,^3\Sigma_g^-(v=0)$ transition at about 9500 cm^{-1}. As already stated, the evolution of band origin $\omega(P, T)$ has already been carefully investigated.[6,7] Here, we would like to understand why the fine structure disappears, why the integrated band intensity increases, and why the ZPL (band-origin exciton + magnon or exciton + vibron + magnon) decreases whereas the phonon sideband (asymmetric broad part of band) increases with rising pressure (see Figure 1).

Therefore, we would like to develop next an adequate model to describe the electronic transition of an oxygen molecule(s) in a compressed environment.

3. Theory

In this absorption process, a pair of neighboring interacting molecules is mainly involved; one molecule performs a pure electronic transition ($^3\Sigma_g^- \rightarrow {}^1\Delta_g$) and a neighboring one, a spin flip because this single electronic transition is only magnetically dipole-allowed. The $^1\Delta_g$ level is narrow whereas the $^3\Sigma_g^-$ level possess a dispersion as a spin excitation because of magnetic interaction, which is spatially anisotropic in α- and δ-O_2. Therefore, the ZPL is revealed in spectra as a doublet, the combined exciton + magnon excitation. The neighboring molecules are also involved in this simultaneous excitation of one exciton, one magnon, one vibron (for the 0−1 transition), and several phonons. In the spectra, a phonon sideband shows up on the higher energetic side of the band origin (exciton + magnon). Because the Δ state has spin $S = 0$, no additional magnons are excited in this process. This magnetic exciton couples with lattice displacements through exchange interaction in the ground state; all other types of intermolecular interactions are less important. In our studies, we applied pressure, which means that the intermolecular distance r is reduced; because the relevant interaction between neighboring molecules is magnetic and because the exchange interaction J is strongly r-dependent, we have to model pressure effects on optical spectra (band-origin ZPL, sideband) as an r-dependence of the actual interactions.

3.1. Hamiltonian of Electronic Excitations of α- and δ-O_2 Interacting with Lattice Phonons. According to our model, this Hamiltonian consists of three relevant terms:

$$H = H_{el} + H_{res} + H_{env}$$

H_{el} describes the pure electronic excitation ($^3\Sigma \rightarrow \Delta$) corresponding to the free molecule, H_{res} takes into account that this molecular excitation is hopping from one molecule to another, and H_{env} considers the main interaction with the environment, in our case, the spin−spin exchange interaction.

As is now well known, the Hamiltonian of magnetic insulators in the case of electronic excitation that possesses only small geometrical extensions can be written in pseudo-spin-vector operators $\sigma_{\mathbf{n}\alpha}$ (**n** is the lattice point, α is the magnetic sublattice index) and formally has the Heisenberg form[15]

$$H_{res} = \frac{1}{2}\sum_{\mathbf{n}\alpha,\mathbf{m}\beta} t_{\mathbf{n}\alpha\mathbf{m}\beta}\sigma_{\mathbf{n}\alpha}\sigma_{\mathbf{m}\beta} \qquad (1)$$

where $t_{\mathbf{n}\alpha\mathbf{m}\beta}$ is the hopping matrix element (of exchange nature) of an electron excitation from the molecule **n**α to the molecule **m**β. The projections $\sigma^X_{\mathbf{n}\alpha}$, $\sigma^Y_{\mathbf{n}\alpha}$, and $\sigma^Z_{\mathbf{n}\alpha}$ differ from spin operator projections $S^X_{\mathbf{n}\alpha}$, $S^Y_{\mathbf{n}\alpha}$, and $S^Z_{\mathbf{n}\alpha}$ by their actions on molecular states: if the latter preserve the value of the total spin, then the former change it by 1. This means that, for instance, that the operator $\sigma_{\mathbf{n}\alpha}$ acting on the ground state with $S = 1$ transfers the molecule in the excited electronic state with $S = 0$ and vice versa. In particular, in O_2 with ground-state spin $S = 1$, one has

$$\sigma^{\pm}_{\mathbf{n}\alpha} = \frac{1}{2}(\sigma^X_{\mathbf{n}\alpha} \pm i\sigma^Y_{\mathbf{n}\alpha}) = \begin{cases} B_{\mathbf{n}\alpha}(-1) - B^+_{\mathbf{n}\alpha}(1) \\ B^+_{\mathbf{n}\alpha}(-1) - B_{\mathbf{n}\alpha}(1) \end{cases} \qquad (2)$$

$$\sigma^Z_{\mathbf{n}\alpha} = B_{\mathbf{n}\alpha}(0) + B^+_{\mathbf{n}\alpha}(0)$$

where the operator $B_{\mathbf{n}\alpha}(S_z)$ with $S_z = \pm 1, 0$ acts on a state with given S_z only from the ground multiplet and creates the singlet excited state. (As mentioned, in O_2 there are two such lowest excited states $^1\Delta_g$ and $^1\Sigma_g^+$.)

If we are interested in the low-temperature absorption spectra, then it is natural to suppose that all transitions take place from the molecular electronic ground state $^3\Sigma_g^-$. Thus, in proper quantization axes, such a state is the one with $S_z = 1$ on each molecule. In these axes, the operator (1) with eq 2 takes the form

$$\begin{aligned} H_{res} &= \frac{1}{2}\sum_{\substack{\mathbf{n},\mathbf{m},\alpha \\ j=X,Y,Z}} t_{\mathbf{n}\alpha\mathbf{m}\alpha}\sigma^j_{\mathbf{n}\alpha}\,\sigma^j_{\mathbf{m}\alpha} + \sum_{\mathbf{n},\mathbf{m}} t_{\mathbf{n}1\mathbf{m}2}(\sigma^X_{\mathbf{n}1}\,\sigma^X_{\mathbf{m}2} + \sigma^Y_{\mathbf{n}1}\,s^Y_{\mathbf{m}2} + \\ &\qquad \sigma^Z_{\mathbf{n}1}\,\sigma^Z_{\mathbf{m}2}) \\ &= \sum_{\substack{\mathbf{n},\mathbf{m},\alpha \\ S_z}} t_{\mathbf{n}\alpha\mathbf{m}\alpha}B^+_{\mathbf{n}\alpha}(S_z)\,B_{\mathbf{m}\alpha}(S_z) - \sum_{\substack{\mathbf{n},\mathbf{m} \\ S_z}} t_{\mathbf{n}1\mathbf{m}2}B^+_{\mathbf{n}1}(S_z)\,B_{\mathbf{n}2}(-S_z) \\ &\quad - \sum_{\mathbf{n},\mathbf{m},\alpha}\left\{ t_{\mathbf{n}\alpha\mathbf{m}\alpha}\left[B_{\mathbf{n}\alpha}(1)\,B_{\mathbf{m}\alpha}(-1) - \frac{1}{2}B_{\mathbf{n}\alpha}(0)\,B_{\mathbf{m}\alpha}(0) + \text{h.c.}\right]\right\} \\ &\quad + \sum_{\mathbf{n},\mathbf{m}} t_{\mathbf{n}1\mathbf{m}2}[B_{\mathbf{n}1}(1)\,B_{\mathbf{m}2}(1) + B_{\mathbf{n}1}(-1)\,B_{\mathbf{m}2}(-1) - \\ &\qquad B_{\mathbf{n}1}(0)\,B_{\mathbf{m}2}(0) + \text{h.c.}] \approx \sum_{\mathbf{n},\mathbf{m},\alpha} t_{\mathbf{n}\alpha\mathbf{m}\alpha}B^+_{\mathbf{n}\alpha}\,B_{\mathbf{m}\alpha} \end{aligned} \qquad (3)$$

with $B_{\mathbf{n}\alpha} \equiv B_{\mathbf{n}\alpha}(1)$. h.c. denotes Hermitian conjugated operator. Consequently, the free exciton Hamiltonian acquires, as seen from eq 3, the simplest form.

The full Hamiltonian (eq 1) generalizes the well-known exciton Hamiltonian for nonmagnetic insulators to the case of magnetic ones. The main contribution (here the first term in eq 3) describes the hopping of the electronic excitation within the molecules of the same magnetic sublattice. The second term with different spin projections describes spin excitations that belong to scattering processes that do not change the absorption intensity, which are therefore neglected here in the absorption spectra. The third term in eq 3 contains double-creation processes (proportional to $B_{\mathbf{n}1}B_{\mathbf{m}2}$), which are small because these processes are proportional to t^2/ϵ, and $\epsilon \gg t$. (ϵ is the energy of the electronic transition $\Sigma \rightarrow \Delta$.[15,16])

In the environmental term H_{env}, the main interaction is the magnetic one in the ground state. In the free molecule, because of spin−orbital interaction the spin-projection degeneracy of the $^3\Sigma_g^-$ ground state is lifted, and the splitting is $A \approx 4$ cm^{-1}

(effectively $H_{anis} = AS_Z^2$).[17] In the solid, because of spin ordering in the α- and δ-phases, the short-range exchange interaction of molecules in the ground state will shift this level by $I \approx 20$ cm^{-1}. The Heisenberg Hamiltonian is

$$H_{exch} = \frac{1}{2}\sum_{\mathbf{n},\alpha,\mathbf{m},\beta} J_{\mathbf{n}\alpha\mathbf{m}\beta}\mathbf{S}_{\mathbf{n}\alpha}\mathbf{S}_{\mathbf{m}\beta} \quad (4)$$

Indeed, in the molecular self-consistent field approximation, this operator has the form

$$H_{exch}^{MF} = -Isz\sum_{\mathbf{n},\alpha} S_{\mathbf{n}\alpha}^{Z} \quad (5)$$

where I is the exchange interaction constant for nearest neighbors, z is the number of neighboring molecules from different magnetic sublattices, and $s \equiv \langle S_{\mathbf{n}\alpha}^{Z}\rangle$ is the mean spin value on each site. The mean field approximation is justified here because we used this approximation only to determine electronic term shifts and not to model excitation energies such as magnons.

When a molecule is excited, its spin $S = 0$ ($^1\Delta_g$ state), and the exchange interaction with neighboring molecules is completely canceled. In other words, this means that an electronically excited molecule is equivalent to a "spin vacancy" (or "spin hole") in the lattice. Naturally, the forces near such a molecule are changed, and some sort of deformation should appear around this molecule. If the lattice is soft enough, then this deformation can follow the electronic excitation ("deformed exciton" or polaron). The peculiarity of this solid consists of the fact that the corresponding interaction of electronic excitations with the lattice is mainly defined by the exchange interaction of molecules in their ground states. This specific interaction then causes the environmental shift of spectral bands in the crystal.

Formally, for calculations, one can use the initial operators (eq 2). At low temperatures, as in our case, only a few phonons/magnons are thermally excited; therefore, it is more convenient to work with exciton operators, considering them to be Bose-type ones. As a result, the final form of the Hamiltonian for crystals with electronic excitation can be written in the form

$$H_{excit} = H_{el} + H_{exch}^{MF} + H_{res} = \epsilon\sum_{\mathbf{n}\alpha} \mathrm{B}_{\mathbf{n}\alpha}^{+}\mathrm{B}_{\mathbf{n}\alpha} - \frac{1}{2}\sum_{\mathbf{n},\alpha,\mathbf{m},\beta} J_{\mathbf{n}\alpha\mathbf{m}\beta} s S_{\mathbf{n}\alpha}^{Z} + \sum_{\mathbf{n},\mathbf{m},\alpha} t_{\mathbf{n}\alpha\mathbf{m}\alpha}\mathrm{B}_{\mathbf{n}\alpha}^{+}\mathrm{B}_{\mathbf{m}\alpha} \quad (6)$$

where the second term in rhs corresponds to the environmental shift $D^{(ex)} = Isz$, and for the sake of simplicity, we can omit H_{anis} because the ratio $A/Isz \leq 0.05$ is sufficiently small.

Having developed now the three terms in the total Hamiltonian in a first step, it is not difficult in a second step to write down the operators of exciton−phonon coupling, taking into account that the intermolecular distance can depend both on electronic excitations and on external parameters—temperature and pressure. Both terms $J_{\mathbf{n}\alpha\mathbf{m}\beta}$ and $t_{\mathbf{n}\alpha\mathbf{m}\alpha}$ can now be expanded in a Taylor series, which means that the molecule $\mathbf{n}\alpha$ is shifted by a vector $\mathbf{u}_{\mathbf{n}\alpha}$ because of vibrations or a pressure effect. In these series, the zero term excludes but the first term includes the simultaneous relaxation of the environment after the molecule $\mathbf{n}\alpha$ is excited:

$$J_{\mathbf{n}\alpha\mathbf{m}\beta} = J_{\mathbf{n}\alpha\mathbf{m}\beta}^{(0)} + \frac{\partial J_{\mathbf{n}\alpha\mathbf{m}\beta}}{\partial|\mathbf{n}\alpha - \mathbf{m}\beta|}(\mathbf{e}_{\mathbf{n}\alpha-\mathbf{m}\beta}, \mathbf{u}_{\mathbf{n}\alpha} - \mathbf{u}_{\mathbf{m}\beta}) \quad \mathbf{e}_{\mathbf{n}\alpha-\mathbf{m}\beta} \equiv \frac{\mathbf{n}\alpha - \mathbf{m}\beta}{|\mathbf{n}\alpha - \mathbf{m}\beta|} \quad (7)$$

(Comments on the fluctuations of the resonance term $t_{\mathbf{n}\alpha\mathbf{m}\alpha}$ are given later.) If the molecules are in fixed positions and in the case of nearest neighbors, we can replace $J_{\mathbf{n1m2}}^{(0)} = I$. In the ground state, there are no excitations (magnons included). After the electronic excitation, the environment relaxes to this new situation (Franck−Condon picture), and new interactions (in the excited state) generate displacements to new molecular equilibrium positions. There are no evident reasons for the appearance of small molecule rotations near an excited molecule both in α- and β-O_2.

The final form of the Hamiltonian with electronic excitations (excitons) and simultaneous phonon relaxation is

$$H_{excit} = \sum_{\mathbf{n}\alpha}(\epsilon + D^{(ex)})\mathrm{B}_{\mathbf{n}\alpha}^{+}\mathrm{B}_{\mathbf{n}\alpha} + \frac{1}{\sqrt{N}}\sum_{\mathbf{n}\alpha}\sum_{\mathbf{q},\nu}\chi_{\mathbf{n}\alpha}^{(\nu)}(\mathbf{q})\,\mathrm{B}_{\mathbf{n}\alpha}^{+}\mathrm{B}_{\mathbf{n}\alpha}\,\varphi_{\nu}(\mathbf{q}) + \sum_{\mathbf{n},\mathbf{m},\alpha} t_{\mathbf{n}\alpha\mathbf{m}\alpha}\mathrm{B}_{\mathbf{n}\alpha}^{+}\mathrm{B}_{\mathbf{m}\alpha} \quad (8)$$

where $\chi_{\mathbf{n}\alpha}^{(\nu)}(\mathbf{q})$ is the exciton−phonon coupling parameter for a phonon of the νth branch with wave vector $\mathbf{q}$; this coupling (see eq 8) is proportional to $\partial J_{\mathbf{n}\alpha\mathbf{m}\beta}/\partial|\mathbf{n}\alpha - \mathbf{m}\beta|$ and the mean spin value s. As usual, $\varphi_{\nu}(\mathbf{q}) = a_{\nu}(\mathbf{q}) + a_{\nu}^{+}(-\mathbf{q})$, with $a_{\nu}(\mathbf{q})$ and $a_{\nu}^{+}(-\mathbf{q})$ being the annihilation and creation phonon operators, respectively.[16]

As already mentioned, the relaxation via magnon excitation in the excited state is not possible ($S = 0$), at least because of the linearity in spin operator terms. If the environment of an excited molecule is relaxing via phonons, then the phonons of the whole density of states (DOS) will be excited. The restriction to the one-phonon DOS (i.e., linearity in phonon operator $\varphi_{\nu}(\mathbf{q})$) is not a principal one. From spectra, we know that the range of the total sideband extends from 1000−1500 cm^{-1} (see Figure 1), so in principle we should consider here several simultaneous multiphonon processes. As a main contribution of this one-phonon excitation, we will consider the "breathing mode" around an excited molecule (symmetry A_g) (i.e., all centers of mass of nearest neighbors will perform an oscillation around their equilibrium positions; therefore, we will consider phonons of longitudinal type only).

It is necessary to stress that the Hamiltonian eq 8 is a strong coupling operator; in that case, exciton−phonon interaction is described by an energy shift term and not by a resonance term (affecting bandwidth). Such an approximation is justified in molecular crystals where usually the former one is larger than the later one.[16] In solid O_2, this means that $|J_{\mathbf{n1m2}}| \gg |t_{\mathbf{n}\alpha\mathbf{m}\alpha}|$, which is confirmed by experiments.[14] The same behavior is observed in collinear magnetic insulators[18,19] where the bandwidth of exciton transitions is narrow and much less than that of exchange interaction.

In this approximation, the main (truncated) part of the Hamiltonian (eq 8), namely,

$$H^{(tr)} = H_{excit}^{(tr)} + H_{ph}$$

$$H_{excit}^{(tr)} = \epsilon_{crys}\sum_{\mathbf{n}\alpha}\mathrm{B}_{\mathbf{n}\alpha}^{+}\mathrm{B}_{\mathbf{n}\alpha} + \frac{1}{\sqrt{N}}\sum_{\mathbf{n}\alpha}\sum_{\mathbf{q},\nu}\chi_{\mathbf{n}\alpha}^{(\nu)}(\mathbf{q})\,\mathrm{B}_{\mathbf{n}\alpha}^{+}\mathrm{B}_{\mathbf{n}\alpha}\varphi_{\nu}(\mathbf{q})$$

$$H_{ph} = \sum_{\mathbf{q},\nu}\omega_{\nu}(\mathbf{q})\,a_{\nu}^{+}(-\mathbf{q})\,a_{\nu}(\mathbf{q}) \quad (9)$$

can be diagonalized by unitary transformation[16]

$$\tilde{H}^{(tr)} \rightarrow e^{\hat{s}}H^{(tr)}e^{-\hat{s}} \quad (10)$$

in which

$$\hat{s} = \sum_{\mathbf{n}\alpha}\sum_{\mathbf{q},\nu} x^{(\nu)}_{\mathbf{n}\alpha}(\mathbf{q})\, \mathrm{B}^{+}_{\mathbf{n}\alpha}\mathrm{B}_{\mathbf{n}\alpha}[a^{+}_{\nu}(-\mathbf{q}) - a_{\nu}(\mathbf{q})] \qquad (11)$$

In eqs 9−11, we use the notions that $\epsilon_{\mathrm{crys}} \equiv \epsilon + D^{(\mathrm{ex})}$ is the pure electronic transition energy in the molecular crystal, $\omega_{\nu}(\mathbf{q})$ is the phonon frequency, and coupling parameters $x^{(\nu)}_{\mathbf{n}\alpha}(\mathbf{q})$ are defined from the condition that the transformed Hamiltonian (eq 10) does not include the linear terms in phonon operators. After some necessary transformations, one can easily come to the expressions

$$e^{\hat{s}}\mathrm{B}_{\mathbf{n}\alpha}e^{-\hat{s}} = \mathrm{B}_{\mathbf{n}\alpha}\exp\left\{\frac{1}{\sqrt{N}}\sum_{\mathbf{q}} x^{(\nu)}_{\mathbf{n}\alpha}(\mathbf{q})[a^{+}_{\nu}(-\mathbf{q}) - a_{\nu}(\mathbf{q})]\right\} \equiv \mathrm{B}_{\mathbf{n}\alpha}e^{-\hat{s}_{\mathbf{n}\alpha}} \qquad (12)$$

$$e^{\hat{s}}\, a_{\nu}(\mathbf{q})\, e^{-\hat{s}} = a_{\nu}(\mathbf{q}) - \frac{1}{\sqrt{N}}\sum_{\mathbf{n}\alpha} x^{(\nu)}_{\mathbf{n}\alpha}(\mathbf{q})\, \mathrm{B}^{+}_{\mathbf{n}\alpha}\mathrm{B}_{\mathbf{n}\alpha}$$

From eq 12, it is seen that when the crystal is not electronically excited (i.e., $\mathrm{B}^{+}_{\mathbf{n}\alpha}\mathrm{B}_{\mathbf{n}\alpha} = 0$) "new" phonon operators are identical to "old" ones, and their difference is proportional to the electronic excitation number $\mathrm{B}^{+}_{\mathbf{n}\alpha}\mathrm{B}_{\mathbf{n}\alpha}$ and the value of $x^{(\nu)}_{\mathbf{n}\alpha}(\mathbf{q})$. Substituting eq 12 in eq 9 gives the next Hamiltonian

$$\tilde{H}^{(\mathrm{tr})} = \tilde{H}^{(\mathrm{tr})}_{\mathrm{excit}} + \tilde{H}_{\mathrm{ph}}$$
$$\tilde{H}^{(\mathrm{tr})}_{\mathrm{excit}} = \tilde{\epsilon}_{\mathrm{crys}}\sum_{\mathbf{n}\alpha}\mathrm{B}^{+}_{\mathbf{n}\alpha}\mathrm{B}_{\mathbf{n}\alpha} \qquad \tilde{H}_{\mathrm{ph}} = H_{\mathrm{ph}} \qquad (13)$$

where

$$\tilde{\epsilon}_{\mathrm{crys}} = \epsilon_{\mathrm{crys}} - \frac{1}{N}\sum_{\mathbf{q}}\frac{|\chi^{(\nu)}_{\mathbf{n}\alpha}(\mathbf{q})|^2}{\omega_{\nu}(\mathbf{q})} \qquad x^{(\nu)}_{\mathbf{n}\alpha}(\mathbf{q}) = \frac{\chi^{(\nu)}_{\mathbf{n}\alpha}(\mathbf{q})}{\omega_{\nu}(\mathbf{q})}$$

which proves to be diagonal. The nondiagonal part in some sense concerns the resonance interaction (eq 9) so that

$$\tilde{H}_{\mathrm{excit}} = \tilde{H}^{(\mathrm{tr})}_{\mathrm{excit}} + \sum_{\mathbf{n},\mathbf{m},\alpha}\hat{t}_{\mathbf{n}\alpha\mathbf{m}\alpha}\mathrm{B}^{+}_{\mathbf{n}\alpha}\mathrm{B}_{\mathbf{m}\alpha} \qquad (14)$$

where the hopping parameter $\hat{t}_{\mathbf{n}\alpha\mathbf{m}\alpha} = \exp(\hat{s}_{\mathbf{n}\alpha} - \hat{s}_{\mathbf{m}\alpha})t_{\mathbf{n}\alpha\mathbf{m}\alpha}$ becomes an operator. In the adiabatic approximation (i.e., vertical transition in the Franck−Condon picture, see ref 16), this last quantity is taken into account without fluctuations due to phonon coupling—contrary to the quantity $J_{\mathbf{n}\alpha\mathbf{m}\beta}$ (eq 7): $\hat{t}_{\mathbf{n}\alpha\mathbf{m}\alpha} = \bar{t}_{\mathbf{n}\alpha\mathbf{m}\alpha} + (\hat{t}_{\mathbf{n}\alpha\mathbf{m}\alpha} - \bar{t}_{\mathbf{n}\alpha\mathbf{m}\alpha}) \approx \bar{t}_{\mathbf{n}\alpha\mathbf{m}\alpha}$, where $\bar{t}_{\mathbf{n}\alpha\mathbf{m}\alpha} = \langle\exp(\hat{s}_{\mathbf{n}\alpha} - \hat{s}_{\mathbf{m}\alpha})t_{\mathbf{n}\alpha\mathbf{m}\alpha}\rangle$ and $\langle ...\rangle$ corresponds to an averaging procedure in the phonon ground state. Because of this averaging procedure, the bandwidth of the polaron is reduced. In such an approximation, one supposes that the resonant hopping of an electronic excitation in the lattice is accompanied by a deformation or "phonon cloud", which corresponds to many-phonon processes.

3.2. Interaction of the Crystal with Light. The dipole transition in solid oxygen in the visible region is described by a double transition. In particular, for exciton−magnon absorption, this second-order operator has the form[14,15]

$$\mathbf{P}^{\mathrm{excit-mag}}_{\mathrm{eff}} = \sum_{\mathbf{n},\mathbf{m}}(\pi_{\mathbf{n}1\mathbf{m}2}\mathrm{B}^{+}_{\mathbf{n}1}\,\mathrm{S}^{-}_{\mathbf{m}2} + hc) \qquad (15)$$

$\mathbf{P}^{\mathrm{excit-mag}}_{\mathrm{eff}}$ is the effective dipole moment. The vector $\pi_{\mathbf{n}1\mathbf{m}2}$ is the dipole moment that describes the transitions of two molecules $\mathbf{n}1$ and $\mathbf{m}2$ from different magnetic sublattices in which the molecule $\mathbf{n}1$ goes over into the electronic state $^1\Delta_g$ and the molecule $\mathbf{m}2$ changes the spin projection. In the dipole approximation, the light-wave vector $\mathbf{Q}$ is equal to zero.

In such a case, the absorption spectrum is described by the imaginary part of the two-particle Green function[20]

$$G(\omega) = \sum_{\mathbf{n},\mathbf{m}}\sum_{\mathbf{p},\mathbf{l}}\pi^{j_1}_{\mathbf{n}1\mathbf{m}2}\,\pi^{j_2}_{\mathbf{p}1\mathbf{l}2}\langle\langle e^{\mathrm{i}Ht}\mathrm{B}_{\mathbf{n}1}\mathrm{S}^{+}_{\mathbf{m}2}e^{-\mathrm{i}Ht};\, \mathrm{B}^{+}_{\mathbf{p}1}\,\mathrm{S}^{-}_{\mathbf{l}2}\rangle\rangle_{\omega} \qquad (16)$$

in which $j_1, j_2 = X, Y, Z, H$ is the basic Hamiltonian, and $\langle\langle ...\rangle\rangle_{\omega}$ corresponds to Fourier transform. But the calculations can be simplified if one uses the transformed operators in eqs 12 and 14. In this case, the initial expression for eq 16 can be approximately decomposed to the form

$$G_{\mathbf{nm},\mathbf{pl}}(t) = -\mathrm{i}\theta(t)\langle[\tilde{\mathrm{B}}_{\mathbf{n}1}(t)\,\mathrm{S}^{+}_{\mathbf{m}2}(t),\, \tilde{\mathrm{B}}^{+}_{\mathbf{p}1}\mathrm{S}^{-}_{\mathbf{l}2}]\rangle \approx -\mathrm{i}\theta(t)\langle e^{\hat{s}_{\mathbf{n}1}(t)}e^{-\hat{s}_{\mathbf{p}1}}\rangle\langle[\tilde{\mathrm{B}}_{\mathbf{n}1}(t)\,\mathrm{S}^{+}_{\mathbf{m}2}(t),\, \tilde{\mathrm{B}}^{+}_{\mathbf{p}1}\,\mathrm{S}^{-}_{\mathbf{l}2}]\rangle \qquad (17)$$

where $\theta(t)$ is the step function and decoupling indicates that additional exciton−phonon interaction coming from the difference $\hat{t}_{\mathbf{n}\alpha\mathbf{m}\alpha} - \bar{t}_{\mathbf{n}\alpha\mathbf{m}\alpha}$ was omitted (i.e., only the operator (eq 14) was taken into account).

As is well known, the second multiplier in eq 17 results in the Debye−Waller factor, which describes the redistribution of intensity between the zero phonon line and the phonon sideband, which, as is well-known, depends only on the exciton−phonon coupling constant $\chi^{(\nu)}_{\mathbf{n}\alpha}(\mathbf{q})$ (see eq 8).

Let us consider this factor; the direct but standard calculation using eq 11 gives

$$\langle e^{\hat{s}_{\mathbf{n}\alpha}(t)}e^{-\hat{s}_{\mathbf{p}\alpha}(t)}\rangle = \left\langle\exp\left\{\frac{1}{\sqrt{N}}\sum_{\mathbf{q},\nu}\frac{\chi^{(\nu)}_{\mathbf{n}\alpha}(\mathbf{q})}{\omega_{\nu}(\mathbf{q})}[a^{+}_{\nu}(-\mathbf{q})\, e^{\mathrm{i}\omega_{\nu}(\mathbf{q})t} - a_{\nu}(\mathbf{q})\, e^{-\mathrm{i}\omega_{\nu}(\mathbf{q})t}]\right\}\right.$$
$$\left.\times\exp\left\{\frac{1}{\sqrt{N}}\sum_{\mathbf{p},\nu}\frac{\chi^{(\nu)}_{\mathbf{p}1}(\mathbf{q})}{\omega_{\nu}(\mathbf{q})}[a_{\nu}(\mathbf{q}) - a^{+}_{\nu}(-\mathbf{q})]\right\}\right\rangle = \exp[g(t)] \qquad (18)$$

$$g(t) = \frac{1}{N}\sum_{\mathbf{q},\nu}\left|\frac{\chi^{(\nu)}_{\mathbf{n}1}(\mathbf{q})}{\omega_{\nu}(\mathbf{q})}\right|^2\{e^{-\mathrm{i}\omega_{\nu}(\mathbf{q})t}[n_{\nu}(\mathbf{q}) + 1] + e^{\mathrm{i}\omega_{\nu}(\mathbf{q})t}n_{\nu}(\mathbf{q}) - [2n_{\nu}(\mathbf{q}) + 1]\}$$

The expression (eq 18) for $g(t)$ is in fact the final one. The only simplification comes from the inequality that usually $T \ll \theta_{\mathrm{D}}$. ($\theta_{\mathrm{D}}$ is the Debye temperature of oxygen of about 100−110 K; the temperature T of the α-O_2 sample is not more than 20 K in our case.) Consequently, we can use $n_{\nu}(\mathbf{q}) = 0$, where $n_{\nu}(\mathbf{q})$ is the phonon occupation number. Then, from eq 18 one has

$$g(t) \approx \frac{1}{N}\sum_{\mathbf{q},\nu}\left|\frac{\chi^{(\nu)}_{\mathbf{n}1}(\mathbf{q})}{\omega_{\nu}(\mathbf{q})}\right|^2[e^{-\mathrm{i}\omega_{\nu}(\mathbf{q})t} - 1] \approx -g_0 + ... \qquad (19)$$

where

$$\exp(-g_0) \equiv \exp\left\{-\frac{1}{N}\sum_{\mathbf{q},\nu}\left|\frac{\chi^{(\nu)}_{\mathbf{n}1}(\mathbf{q})}{\omega_{\nu}(\mathbf{q})}\right|^2\right\}$$

is the ZPL intensity I_{ZPL}, which we are interested in.

In the next paragraph, we find the pressure dependence of this value $I_{ZPL}(P)$ with respect to the above-described excitation (exciton + magnon in a pair of molecules) and simultaneous relaxation of neighboring molecules. The coupling parameter $\chi^{(\nu)}_{\mathbf{n}\alpha}(\mathbf{q})$ for the α- and δ-O_2 lattices (the monoclinic layered structure with a very weak exchange interaction between layers) can be written in the form

$$\chi^{(\nu)}_{\mathbf{n}\alpha}(\mathbf{q}) = \frac{1}{\sqrt{N}} \sum_{\mathbf{m}\beta(\neq\alpha)} \chi_{\mathbf{n}\alpha\mathbf{m}\beta} s \sqrt{\frac{\hbar}{2M\omega_\nu(\mathbf{q})}} (\mathbf{e}_\nu(\mathbf{q})\mathbf{e}_{\mathbf{n}\alpha-\mathbf{m}\beta}) e^{i\mathbf{q}\mathbf{n}\alpha} [1 - e^{-i\mathbf{q}(\mathbf{n}\alpha-\mathbf{m}\beta)}]$$

$$= \frac{2i}{\sqrt{N}} \chi(\rho) s \sqrt{\frac{\hbar}{2M\omega_\nu(\mathbf{q})}} F_\nu(\mathbf{q}) e^{i\mathbf{q}\mathbf{n}\alpha} \quad (20)$$

$$F_\nu(\mathbf{q}) = \frac{\mathbf{a}\mathbf{e}_\nu(\mathbf{q})}{2\rho} \sin \mathbf{q}\frac{\mathbf{a}}{2} \cos \mathbf{q}\frac{\mathbf{b}}{2} + \frac{\mathbf{b}\mathbf{e}_\nu(\mathbf{q})}{2\rho} \sin \mathbf{q}\frac{\mathbf{b}}{2} \cos \mathbf{q}\frac{\mathbf{a}}{2}$$

where the vector $\rho = \pm(\mathbf{a} \pm \mathbf{b})/2$ corresponds to the nearest-neighbor distance in the *ab* plane and **a** and **b** are the lattice parameters. In eq 20, M is the O_2 molecular mass, and $\mathbf{e}_\nu(\mathbf{q})$ is the acoustic wave polarization. As we previously described, the main contribution to this relaxation process is a breathing mode (i.e., all nearest neighbors in the *ab* plane perform a translational motion of their centers of mass around their equilibrium positions). Consequently, all nearest neighbors couple to the excited pair of molecules via the same coupling coefficient $\chi(\rho)$ and from all phonons only longitudinal waves contribute to the form factor $F_\nu(\mathbf{q})$, or $\nu \equiv l$. (F_l is dimensionless, a constant close to 1, and independent of pressure.) Longitudinal acoustic phonons are described by the following dispersion law

$$\omega_l(\mathbf{q}) = c_l q$$

In the long-wavelength approximation ($q \rightarrow 0$), the value

$$c_l \approx \xi \sqrt{\frac{1}{M} \frac{\partial^2 V}{\partial r^2}|_{r=\rho}} \rho$$

is the longitudinal phonon velocity. (V is the intermolecular interaction, and ξ is a coefficient approximately equal to 1.) As a result, the ZPL intensity is defined by the equation

$$I_{ZPL} \approx \exp\left(-\frac{1}{N}\sum_{\mathbf{q}} \frac{4\chi^2(\rho)}{2M\,\omega_l^3(\mathbf{q})\,\hbar} F_l^2(\mathbf{q})\right) \approx \exp\left(-\frac{\chi^2(\rho)\,\rho^3}{\hbar M c_l^3} F_l^2\right) \quad (21)$$

As was described before, the main contribution—or peculiarity of this solid—to this intermolecular interaction of electronic excitations with the lattice is the exchange interaction of molecules in their ground state. Therefore, for a simple estimation, we write $V(\mathbf{r}) \approx J(\mathbf{r})$ and $\chi(\rho) \approx \partial J(\mathbf{r})/\partial r$ (see eq 8); consequently, we get for the actual argument in the exponent in eq 21

$$\frac{\chi^2(\boldsymbol{\rho})\rho^3}{\hbar M c_l^3} = \frac{(\partial J(\mathbf{r})/\partial r)^2 \rho^3}{\hbar M c_l^3} = \frac{\sqrt{M}}{\hbar \xi^3} \frac{(\partial J(\mathbf{r})/\partial r)^2}{(\partial^2 J(\mathbf{r})/\partial r^2)^{3/2}} \equiv \zeta \quad (22)$$

Of course, $V(r)$ is the total potential, and $J(r)$ the exchange part only. Here as was said before we use $V(\mathbf{r}) = J(\mathbf{r})$ only to be able to perform an estimation of its pressure dependence. Otherwise, these expressions would be too complex.

3.3. Effect of Pressure. Nowadays, it is commonly accepted to model the exchange interaction by the following expression:[7,21]

$$J(\rho) = J_0 \exp[-\alpha(\rho - \rho_0)]$$

$J_0 = 19.6\ \text{cm}^{-1}$, $\alpha = 3.765\ \text{Å}^{-1}$, and $\rho_0 = 3.187$ Å. If we insert this expression into eq 22, we get

$$\zeta = \sqrt{M}(\hbar\alpha\xi^3)^{-1}\sqrt{J(\boldsymbol{\rho})}$$

Applying pressure, the intermolecular distance in the *ab* plane varies according to the phenomenological dependence[22]

$$\rho(P) = \left[\frac{x}{(1 + yP)}\right] + z$$

with parameters $x = 0.838$ Å, $y = 0.00256\ \text{GPa}^{-1}$, and $z = 2.348$ Å, which fit the experimental data. So, the parameter ζ (eq 22) is described by the following expression:

$$\zeta = \sqrt{MJ_0}(\hbar\alpha\xi^3)^{-1} \exp\left(-\frac{1}{2}\alpha\left(\left[\frac{x}{(1 + yP)}\right] + z - \rho_0\right)\right) \quad (23)$$

4. Comparison of Experiment and Theory

Consequently, from our theoretical model, we expect a decrease of the ZPL intensity with increasing pressure (see eq 23)

$$I_{ZPL}(P) \approx e^{A \exp(f(\rho))} \quad (24)$$

As we have already described, the effect of pressure on the spectra was three-fold: the two bands as a whole increase, the ZPL component decreases, and the phonon sideband increases with pressure. Therefore, we have to deconvolute the complex spectra first according to different kinds of excitations such as exciton, vibron, phonon, and magnon. In addition, we have to consider in this combined excitation also the Stokes part (pure intramolecular transition plus lattice excitations) and the anti-Stokes part (pure intramolecular transition minus lattice excitation); the later one is negligible at these low temperatures. The large asymmetry of each band is due to multiphonon process excited at low temperatures. Details of the modeling of this deconvolution were described in ref 6. In short (see Figure 2), one band is now modeled by three components (i.e., two Gaussian functions for the exciton−magnon doublet and an analytical function for the Stokes part of the phonon sideband (asymmetric double-sigmoidal function)). The deconvolution is now applied to all spectra in Figure 1.

For further analysis of the integrated intensities I_{ZPL}, we have to take into account that the spectra at ambient pressure are taken from a sample with thickness 1.2 mm, and the ones at elevated pressure are taken from samples in the high-pressure cell (thickness 50 μm). The absorption process ($^3\Sigma^3\Sigma \rightarrow \Delta^3\Sigma$) can be described by the standard Lambert's law, which contains the absorption coefficient for this electronic transition and sample thickness; we assume the latter one to be independent of pressure. The result is shown in Figure 3, where a decrease of the integrated intensity I_{ZPL} is demonstrated. Because we are interested only in the relative change in the band intensity with pressure, we plotted the ratio $I_{ZPL}(P)/I_{ZPL}(P = 0)$.

Next, we discuss the influence of pressure on band shape: first, the intensity $I_{ZPL}(P)$ (Figure 3); second, the splitting (Figure 4); and third, the total band intensity (Figure 5).

The solid line in Figure 3 describes the theoretically expected behavior due to eq 24; experimental data points are derived from

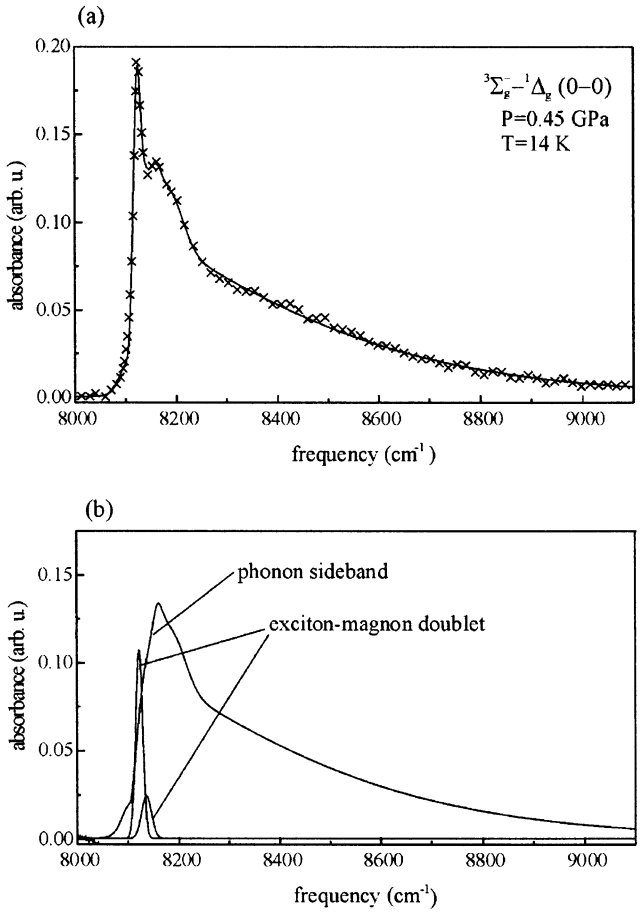

Figure 2. Determination of band origin. (a) The original spectrum (×) is modeled by three bands (—). (b) Components of the synthetic spectrum. The small contributions of negative frequencies of the ZPL are due to the anti-Stokes component of the phonon sideband. The fact that the intensity of the phonon sideband is not zero at the ZPL frequency is due to multiphonon processes (i.e., creation/annihilation of phonons).

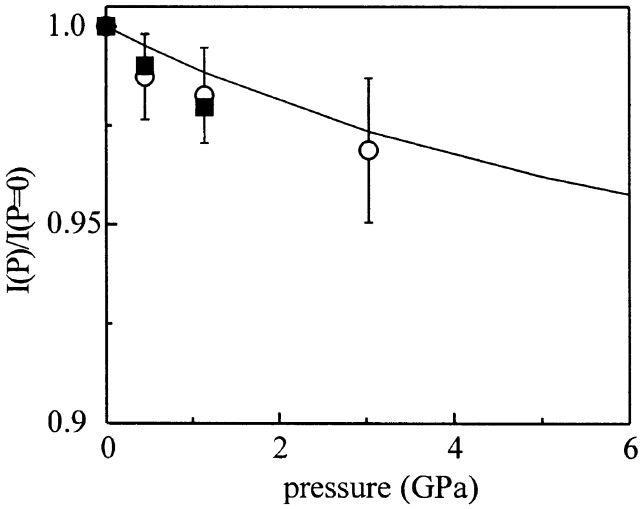

Figure 3. Scaled integrated intensity of band origin I_{ZPL} (exciton/magnon doublet) as a function of pressure. (■) transition $\Sigma \rightarrow \Delta(0)$, (○) transition $\Sigma \rightarrow \Delta(1)$, (—) from theory (eq 21). The error bars correspond to statistical errors of the deconvolution process.

deconvoluted spectra for both double transitions ($^3\Sigma^3\Sigma \rightarrow \Delta$-$(0)^3\Sigma$, $\Delta(1)^3\Sigma$, where 0 and 1 correspond to vibron numbers). Although error bars of experimental points are a few percent, the agreement with the theoretical line is well documented. The

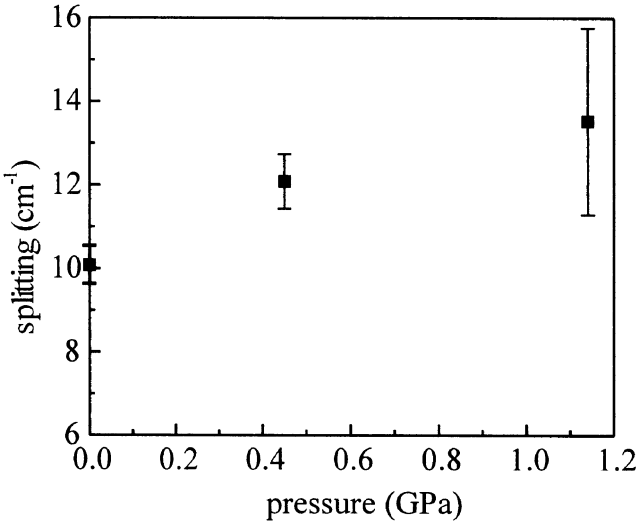

Figure 4. Splitting of exciton−magnon doublet for the transition $\Sigma \rightarrow \Delta(1)$ as a function of pressure. The error bars are due to the statistical error of the deconvolution process.

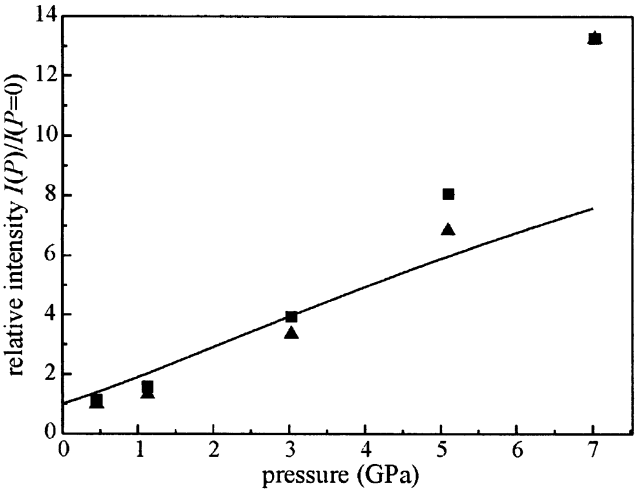

Figure 5. Total integrated intensity of both transitions from spectra in Figure 1 as a function of pressure: (■) $\Sigma \rightarrow \Delta(0)$, (▲) $\Sigma \rightarrow \Delta(1)$, (—) theoretical expectation (see the text).

decrease of $I_{ZPL}(P)$ can be explained qualitatively as follows: Applying pressure means reducing the distance between molecules. The electronic excitation of a pair of molecules, as it takes place also in ordinary single-molecule transitions, is not a direct (vertical) transition in the Franck−Condon picture but an indirect one (slightly inclined) because the pure electronic transition in a pair of molecules is accompanied by a relaxation of the surrounding. Consequently, the overlap of the final and initial vibrational wave functions of the molecules is decreasing, or $I_{ZPL}(P)$ is decreasing. Therefore, because of the Debye−Waller factor, there will be a redistribution of band intensity from the zero phonon band to the sideband.

The two first peaks of the fine structure are situated at 7988.3/8003.7 cm^{-1} in the spectrum $^3\Sigma_g^-(0)^3\Sigma_g^-$ (0) → $^1\Delta_g(0)^3\Sigma_g^-$ (0) and at 9471.1/9480.8 cm^{-1} in the spectrum $^3\Sigma_g^-(0)^3\Sigma_g^-$ (0) → $^1\Delta_g(1)^3\Sigma_g^-(0)$ at ambient pressure and at $T = 14$ K. We could follow this splitting at high pressure only for the second transition (see Figure 1); therefore, we plotted this splitting only for this transition in Figure 4. According to ref 14, we assigned this doublet at the band origin to the simultaneous creation of a $^3\Sigma_g^-(0)^3\Sigma_g^-$ (0) → $^1\Delta_g(1)^3\Sigma_g^-(0)$ exciton + vibron in one molecule (i.e., the frequency of the absorbed photon equals the

sum of exciton + vibron and magnon frequencies at Brillouin zone boundaries). The sharp profile of these doublets are caused by singularities of the magnon density of states at two points in **k** space: $\boldsymbol{k}_1 \perp \mathbf{a}$, $\boldsymbol{k}_1 \approx \pi/b$, and $\boldsymbol{k}_2 \perp \mathbf{b}$, $\boldsymbol{k}_2 \approx \pi/a$ (**a** and **b** are vectors of the unit cell in the basal plane of the α-phase). Now, if pressure is applied to the oxygen crystal, the basal plane is deformed such that the b/a ratio increases by about 10% in that pressure range.[10,23] As a consequence of this increase in structural anisotropy, the magnon frequencies in both directions of the basal plane increase; therefore, this splitting also increases.

In the paper by Gaididei et al.,[14] we found a justification of our qualitative picture in which they determined theoretically the frequency splitting of this doublet at ambient pressure. They calculated the absorption coefficient for this transition ($^3\Sigma_g^-{}^3\Sigma_g^- \rightarrow {}^1\Delta_g{}^3\Sigma_g^-$) and found two maxima at two different light frequencies for the transition of the dipole moment along and across ($\omega_{||}$, $\omega_\perp$) the monoclinic axis b of the crystal. The frequency splitting $\Delta\omega$ has two contributions: one from the resonance interaction ($L \approx t_{\mathbf{n}\alpha\mathbf{m}\alpha}$) and one from the exchange interaction I between nearest neighboring molecules of one sublattice

$$\Delta\omega = \omega_\perp - \omega_{||} = 4(L + I) \approx 10\ \mathrm{cm}^{-1}$$

Because the electron−vibron excited level ($^1\Delta_g(1)$) has no dispersion ($L \ll I$) and since the exchange interaction J_{n1m2} between nearest molecules of different magnetic sublattices plays no role here, we have to consider only $\Delta\omega \approx I$, which is influenced by pressure, as we did it qualitatively before. Because the pressure dependence of $I(\rho)$ is not known in the literature and because we possess only three data points for $\Delta\omega(P)$, we are not able to continue the comparison of experiment and theory.

Figure 5 shows the increase of the total band intensity with pressure for both transitions (■, $^3\Sigma \rightarrow \Delta(0)$; ▲, $^3\Sigma \rightarrow \Delta(1)$), which is mostly generated by the Stokes part of the phonon sideband: $I_{abs} = I_{ZPL} + I_{SB} \approx I_{SB}$. A similar result was found by Medvedev et al. (see Figure 7 in ref 6, where the integrated intensities of the same transitions were plotted as a function of temperature). Lowering the temperature is in this context a similar effect to raising the pressure, but much smaller. In general, the intensity of a sideband is proportional to a coupling between intermolecular excitations (e.g., excitons, vibrons) and lattice excitations multiplied by the phonon density of states. As was pointed out above, this electronic excitation−phonon coupling parameter χ in solid oxygen is proportional to $\partial J(r)/\partial r$ (see eqs 8 and 9), so for the exciton−magnon band, $I_{SB} \approx \chi \cdot \mathrm{DOS} \approx \partial J(r)/\partial r$. Because the exchange integral $J(r)$ between molecules in different magnetic sublattices is known in the literature[7,24] we can plot this value $\partial J(r)/\partial r$ for comparison in Figure 5. The deviation between experimental values (■, ▲) and theory (—) at pressure $P > 5$ GPa can be explained by the influence of two effects: because the total phonon sideband extends in our spectra up to 1000 cm^{-1}, multiphonon process and not only one phonon density of states should be taken into account. In addition but less important is the pressure broadening of the phonon DOS

Finally, we stress an experimental finding of certain more general relevance. Because we measured double $^3\Sigma^3\Sigma \rightarrow \Delta(0)^3\Sigma$ and $^3\Sigma^3\Sigma \rightarrow \Delta(1)^3\Sigma$ transitions, we can deduce the frequency of the vibron excitation in the first electronic state, which shows this frequency significantly softening in the δ-phase because of pressure (see Figure 7d in ref 24). We interpret this nontrivial result as a reduction in the stability of the electronic structure of the magnetically ordered δ-phase by an increase in pressure. This vibron softening in the electronic ground state is well known in solid hydrogen[25] and in solid iodine[26] and is associated there with a precursor for the insulator−metal transition.

5. Conclusions

We analyzed experimentally and theoretically the influence of pressure on the optical band shape of double electronic transitions in solid oxygen α- and δ-phases. The aim was to understand the influence of spin−spin exchange interaction on different types of elementary excitations.

From electronic spectra, we intended to derive integrated intensities; therefore, it was mandatory to produce samples at ambient and elevated pressure with good optical quality, even at low temperatures. Although the absorption spectra in the near-visible region were quite complex, we were able to suggest an unambiguous assignment (combined excitation of exciton, vibron, magnon, and phonon). We deconvoluted these spectra into a zero phonon line and a phonon sideband and plotted the exciton−magnon splitting (Figure 4), the intensity of ZPL (Figure 3), and the total intensity as a function of pressure (Figure 5).

Finally we compared these three experimental results with a theoretical model (i.e., an electronic transition in one molecule and a spin flip in a neighboring one, in combination with a simultaneous relaxation of neighboring molecules that interact magnetically): (i) The intensity of ZPL decreases with rising pressure because the equilibrium positions of molecules in the ground and excited states are shifted. (ii) The exciton−magnon splitting increases with pressure because the anisotropy of the basal plane increases. (iii) The total band intensity increases with pressure because the combined excitations are assisted by exchange intermolecular interaction.

Acknowledgment. We thank Dr. A. Brodyanski for stimulating discussions. This work was supported by the Deutsche Forschungsgemeinschaft (grant Jo 86/10-1) and by EU contract no. HPR ICT 1999-00111. V.L. appreciates the support by German Academic Exchange Service (DAAD) for the opportunity to carry out this research work at the University of Kaiserslautern, and H.J.J. appreciates the funding of a research stay at LENS by INFM.

References and Notes

(1) Amaya, K.; Shimizu, K.; Eremets, M. I.; Kobayashi, T. C.; Endo, S. *J. Phys. C* **1998**, *10*, 11179.

(2) Nicol, M.; Hirsch, K. R.; Holzapfel, W. B. *Chem. Phys. Lett.* **1979**, *68*, 49. Nicol, M.; Syassen, K. *Phys. Rev. B* **1983**, *28*, 1201.

(3) Desgreniers, S.; Vohra, Y. K.; Ruoff, A. L. *J. Phys. Chem.* **1990**, *94*, 1117.

(4) Shimizu, K.; Suhara, K.; Ikumo, M.; Eremets, M.; Amaya, K. *Nature* **1998**, *393*, 767.

(5) Loktev, V. M. *Low Temp. Phys.* **2000**, *26*, 932.

(6) Medvedev, S. A.; Brodyanski, A. P.; Jodl, H. J. *Phys. Rev. B* **2001**, *63*, 184302.

(7) Santoro, M.; Gorelli, F. A.; Ulivi, L.; Bini, R.; Jodl, H. J. *Phys. Rev. B* **2001**, *64*, 64428.

(8) Gorelli, F.; Ulivi, L.; Santoro, M.; Bini, R. *Phys. Rev. B* **2000**, *62*, R3604.

(9) Freiman, Y.; Jodl, H. J. *Phys. Rep.* In press.

(10) Gorelli, F.; Santoro, M.; Ulivi, L.; Hanfland, M. *Phys. Rev. B* **2002**, *65*, 172106.

(11) Gorelli, F.; Santoro, M.; Ulivi, L.; Bini, R. *Phys. Rev. B* **2001**, *63*, 104110.

(12) Neaton, J. B.; Ashcroft, N. W. *Phys. Rev. Lett.* **2002**, *88*, 205503.

(13) Bini, R.; Ballerini, R.; Pratesi, G.; Jodl, H. J. *Rev. Sci. Instrum.* **1997**, *68*, 3154. Gorelli, F.; Santoro, M.; Ulivi, L.; Bini, R. *Phys. Rev. Lett.* **1999**, *83*, 4093.

(14) Gaididey, Yu. B.; Loktev, V. M.; Prikhot'ko, A. F.; Shanskii, L. I. *Zh. Eksp. Teor. Fiz.* **1975**, *68*, 1706 [*Sov. Phys. JETP* **1975**, *41*, 855.].

(15) Gaididei, Yu. B.; Loktev, V. M.; Prikhot'ko, A. F. *Sov. Low Temp. Phys*. **1977**, *3*, 549.

(16) Davydov, A. S. *Theory of Molecular Excitons*; McGraw-Hill: New York, 1962.

(17) Wachtel, E. J.; Wheeler, R. G. *J. Appl. Phys.* **1971**, *42*, 1581.

(18) Eremenko, V. V. *Introduction in the Optical Spectroscopy of Magnets*; Naukova Dumka: Kiev, 1975 (in Russian).

(19) Eremenko, V. V.; Litvinenko, Yu. G.; Matyushkin, E. V. *Phys. Rep.* **1986**, *132*, 55.

(20) Loudon, R. *Adv. Phys.* **1968**, *17*, 243.

(21) Sumarokov, V. V.; Freiman, Yu. Y.; Manzhelii, V. G.; Popov, V. A. *Fiz. Nizk. Temp. (Kiev)* **1980**, *6*, 1195. [*Sov. J. Low Temp. Phys.* **1980**, *6*, 580.]

(22) Gorelli, F.; Santoro, M.; Ulivi, L.; Hanfland, M. Unpublished data.

(23) Akahama, Y.; Kawamura, H. *Phys. Rev. B* **2001**, *64*, 54105.

(24) Brodyanski, A.; Medvedev, S.; Minenko, M.; Jodl, H. J. In *Frontiers of High-Pressure Research II: Application of High Pressure to Low-Dimensional Novel Electronic materials*; Hochheimer, H. D., Kuchta, B., Dorhout, P. K., Yarger, J. L., Eds.; NATO Science Series; Kluwer Academic Publishers: Dordrecht, The Netherlands, 2001.

(25) Hemley, R. J.; Soos, Z. G.; Hanfland, M.; Mao, H.-k. *Nature* **1994**, *369*, 384.

(26) Congeduty, A.; Postorino, P.; Nardone, M.; Buontempo, U. *Phys. Rev. B* **2002**, *65*, 014302.